ChemComm

Accepted Manuscript

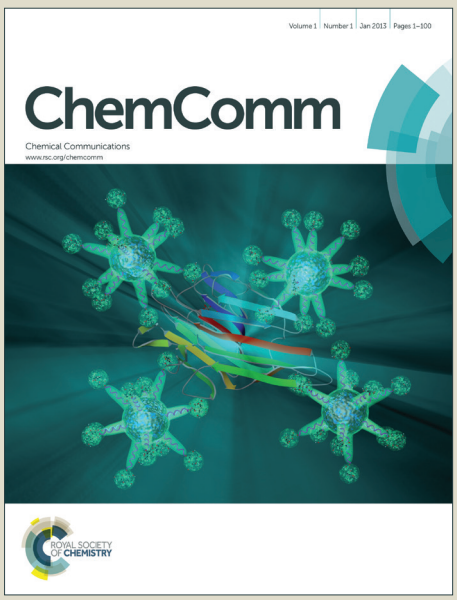

ROYAL SOCIETY OF CHEMISTRY

www.rsc.org/chemcomm

Journal Name

RSCPublishing

COMMUNICATION

Exclusive self-aligned β-phase PVDF films with abnormal piezoelectric coefficient via phase inversion

Cite this: DOI: 10.1039/x0xx00000x

N. Soin,[a,*,†] D. Boyer,[b,†] K. Prashanthi,[c] S. Sharma,[d] A. A. Narasimulu[a], J. Luo[a,*], T. Shah[a], E. Siores [a] and T. Thundat[c]

Received ooth January 2012,
Accepted ooth January 2012

DOI: 10.1039/x0xx00000x

www.rsc.org/

Self-polarised poly(vinylidene fluoride), (PVDF) films were prepared via facile phase-inversion technique wherein the polymorphism of the films was controlled from exclusive α-(>90%) to β-phase (>98%) by simply varying the quenching temperature from 100 °C to -20 °C, respectively. At low temperatures, the β-phase crystallites were found to be self-aligned, with the PVDF thin films possessing high piezoelectric coefficient of up to -49.6 pm/V. The extraordinarily high β-phase and piezoelectric coefficient of these PVDF films makes them suitable for electroactive and energy harvesting applications.

Poly(vinylidene fluoride), (PVDF), is one of the most attractive polymers owing to its remarkable pyro-, piezo- and ferro-electroactive properties.[1-4] These properties stem from its unique polymorphism which gives rise to its extraordinary mechanical properties, high thermal, chemical stability and biocompatibility.[5] Among the four significant crystalline phases α, β, δ and γ; [2, 6] the electroactive β-phase is most utilized for sensing, actuation [7,8] and microgenerator applications.[4,9,10] Various methods for crystallisation of β-phase have been investigated including melt casting,[15] solution deposition,[11, 12] spin coating[13] and phase inversion.[14,15] While, the PVDF films formed by melting/crystallisation are dominated by α-phase;[16] those obtained by spin-coating and dried at temperatures between 30-60 ºC are primarily β-phase.[13] During phase inversion, the PVDF films are formed by rapidly quenching the cast films into a non-solvent bath to induce liquid-solid and liquid-liquid phase separation events.[5,14,15] The microstructure and crystalline phase is controlled by adjusting parameters like composition,[5,13] solvent type,[17,18] quenching temperature etc.[19,20] The PVDF films thus formed show random orientation of β-phase crystals and are mostly porous and hence unsuitable for electroactive applications. To obtain electroactive films, polarisation at high electric field,[6,21] by corona poling,[13] or by mechanical stretching[3,6,16] are required. Recently, self-polarisation of oriented β-phase crystals has been observed in ultrathin co-polymer PVDF films formed by spin-coating[22] and Langmuir-Blodgett (LB)[23,24] method, and has been attributed to the built-in electric field,[22] in-film stress and the strong interaction of PVDF molecules with polar water.[23,24] Similarly, PVDF mesoscale rod arrays and γ-phase PVDF nanofibers formed by drawing were reported to possess good piezoelectric properties.[25, 26] For both these cases, mechanical stretching and stress during template guiding are believed to be responsible for the enhanced piezoelectric effect. Here, we report on the facile preparation of self-polarised β-phase, high piezoelectric coefficient PVDF films *via* phase inversion at low temperatures for electroactive applications. PVDF films were produced using a 30 wt.% PVDF, N,N-Dimethylformamide (DMF) solution. A fixed volume of the as-prepared solution was then deposited on highly polished glass slides *via* spin-coating process. The spin-coated films were immersed immediately in deionized water bath held at various quenching temperatures, T_Q, for 30 min to remove DMF. Further experimental details can be found in the Supporting Information (SI).

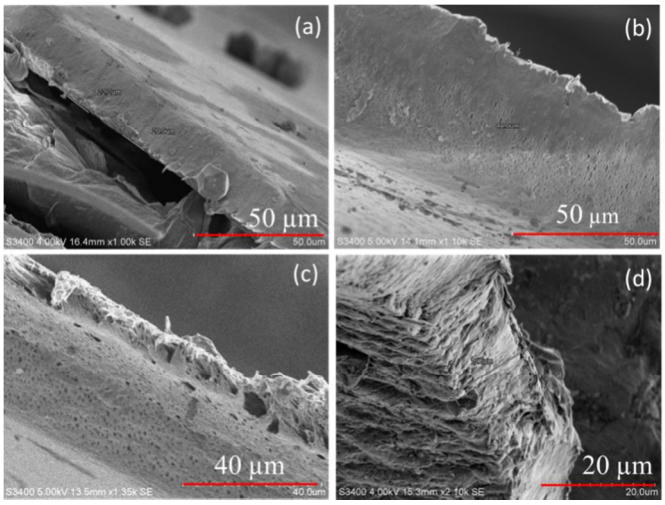

Fig. 1 SEM images of the free-standing PVDF films after quenching at temperatures of a) -20 ºC, b) -5 ºC, c) 40 ºC, and e) 100 ºC.

As seen in figure 1(a-d), the film thickness varied between 20-45 µm, strongly dependent on the T_Q, with quenching at higher temperatures accelerating the liquid-liquid demixing process, leading to films with lower thicknesses.[5,18] The films formed at $T_Q \geq 0$°C have two distinct top dense and low porous regions. The porosity of the films decreases with the decrease in quenching temperature as observed by others.[5,18,20] This is attributed to the slow crystallization and elimination of the DMF owing to the decreased miscibility and mobility of DMF at lower temperatures. Films quenched at -20ºC appear to be very dense with almost no pores of visible sizes. The low quenching temperature and high PVDF concentration are believed to be responsible for this reduced porosity.

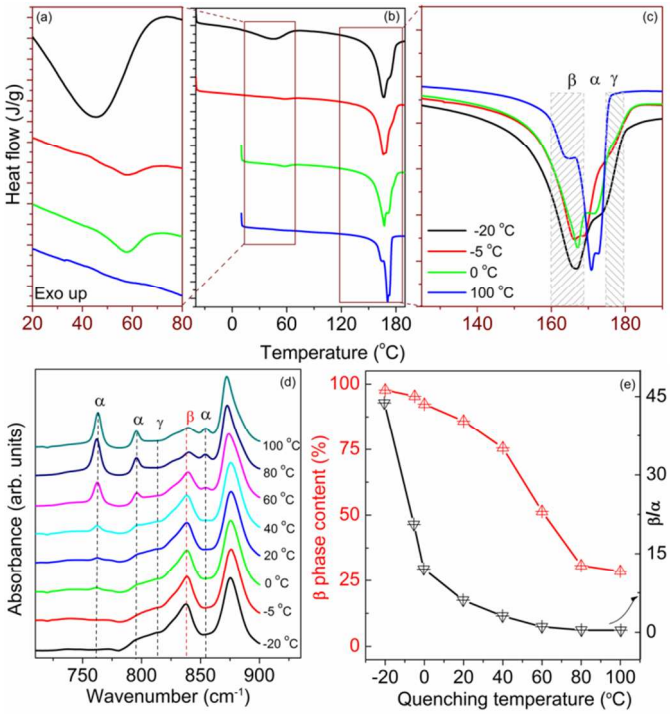

Fig. 2 DSC themograms showing (a) the upper glass transition, (b) melting peaks and (c) their assignment for various crystalline phases; (d) FTIR spectra; (e) β-phase content, β/α ratio as a function of quenching temperature.

The differential scanning calorimetry thermograms for PVDF films are shown in figure 2(a-c). The PVDF films show a melting temperature, T_M, in the range of 165-170ºC, with shoulder-like structures appearing at both low and high temperature sides for all samples. The T_M of the films quenched at -20ºC is 166.5ºC, which is approximately 5ºC lower, as compared to that of 170.9 ºC for films quenched at 100ºC. This lowering of T_M is attributed to the enhanced β-phase content and the reduced porosity of the films.[27,28] It is largely accepted in the literature that β-phase melting occurs in the range 165-172ºC; α-phase crystals in the range 172-175ºC with the γ-phase melting between 175-180ºC (marked in fig 2c).[10,27] The thermogram for sample quenched at 100ºC is largely enclosed within the range of 170-175ºC, corresponding to the dominant α-phase. Similarly, for samples quenched at T_Q<40ºC, a clear shift of the melting peak towards the lower temperature, corresponding to the dominant β-phase can be observed. The total crystallinity of samples, ΔX_C, can be calculated by assuming the fusion heat of 100% crystalline PVDF to be 104.7 J/g. [29]

$$\Delta Xc = \frac{\Delta Hm}{\Delta Hm100} \times 100\% \quad (1)$$

where ΔH_m and ΔH_{m100} are the melting enthalpy of the sample and the melting enthalpy for a 100% crystalline sample, respectively. With the reduction in T_Q, the crystallinity values increase almost linearly from 38.6% (starting pellets) to ~43.3% (T_Q 100ºC) to nearly 56.0% (T_Q -20ºC), which is significantly higher than the typical values of 40-45%, obtained by other methods.[3,16] This increase in the crystallinity can be attributed to the slow liquid-liquid demixing process, reducing the mass exchange between solvent and non-solvent providing more time for crystallisation and enhancement of β-phase.[5] Further small endothermic peaks were observed in the range of 45-60ºC (Figure 2a) for samples quenched at T_Q<20ºC, which disappeared for samples quenched at higher temperatures (T_Q>40ºC). These peaks are attributed to the upper glass transition[30] reorganisation within conformationally disordered α-crystals,[31] or melting of paracrystalline domains within the PVDF films.[32]

The Fourier transform infrared spectroscopy (FTIR) of the PVDF films is shown in Figure 2(d). The appearance of bands at 760, 796, 975, 1210, 1383 and 1423 cm^{-1} are ascribed to the formation of the α-phase[11]; while peaks observed at 840 and 1234 cm^{-1} are ascribed to the β-phase crystallites.[11,27] The quantification of the relative α- and β-phases (Fig. 2(e)) was carried out using the following relationship[3, 6, 27 33]

$$F_\beta = \frac{X_\beta}{X_\alpha + X_\beta} = \frac{A_\beta}{1.26A_\alpha + A_\beta} \quad (2)$$

where A_α and A_β are absorption bands at 760 cm^{-1} and 840 cm^{-1}, respectively. For sample quenched at T_Q<0ºC, the α-peak was completely suppressed giving rise to pure (>98%) β-phase film further corroborated by DSC and XRD measurements (see SI).

Figure 3(a-d) shows the piezoelectric response for samples quenched at -20 and 100 ºC respectively measured by piezoresponse force microscopy (PFM) for a scan size of 50 µm x 50 µm, under an AC bias of 3V. The topography of the PVDF films shows spherical structures, which are representative of a crystallisation-dominated precipitation, wherein all the crystalline particles are nucleated in a similar concentration field and fused together to form a bi-continuous structure.[18] Although the surfaces are relatively rough (roughness ~150 nm), they are suitable for the fabrication of electric devices, as even at a low excitation signal of 3V large piezoelectric response was clearly observed. These results demonstrate that the films quenched at low temperatures not only have a high β -phase content, but also are self-aligned and polarised. The PFM calibration process, carried out in accordance with previous reports, and further calculation of d_{33} coefficients is provided in the supporting information.[33-35] The d_{33} value increases with the decrease in quenching temperature, reaching ~49.6 pm/V, much higher than the typical values of -20 to -35 pm/V of commercial products and those obtained by mechanical stretching and subsequent poling (Fig. 4a).[3,6,21,36] These values are comparable to the PVDF nanofibres which show a d_{33} coefficient of -54 pm/V, which originates from the extraordinarily high γ-phase with ~75% crystallinity.[26] It our case, the piezoelectric response was measured using local excitation

method in which the electromechanical vibrations are induced by the application of an AC voltage between the bottom electrode and the conductive AFM tip to probe the polarisation distribution in the film. The method offers high lateral resolution and correlation between ferroelectric domains and film morphology. However, in this case, the electric field generated by the AFM tip is highly inhomogeneous, making the quantitative analysis of field-induced signal extremely difficult.[35] Thus, PFM measurements without the extended top electrode collects signal only from a surface layer of an unknown thickness, which is a function of dielectric permittivity and contact conditions and the PFM amplitude response essentially originates only several nanometres below the surface which makes the measurement surface sensitive.[33-35] In our case, the abnormally high piezoelectric coefficient from the films quenched at -20ºC is attributed to the exclusive (~100%) β-phase content, extremely high crystallinity of 56% and β/α ratio of 45, all of which are much higher than typical values of 75-85%, <45% and <8, respectively, of commercial products and those reported by various other groups.[3,5,16]

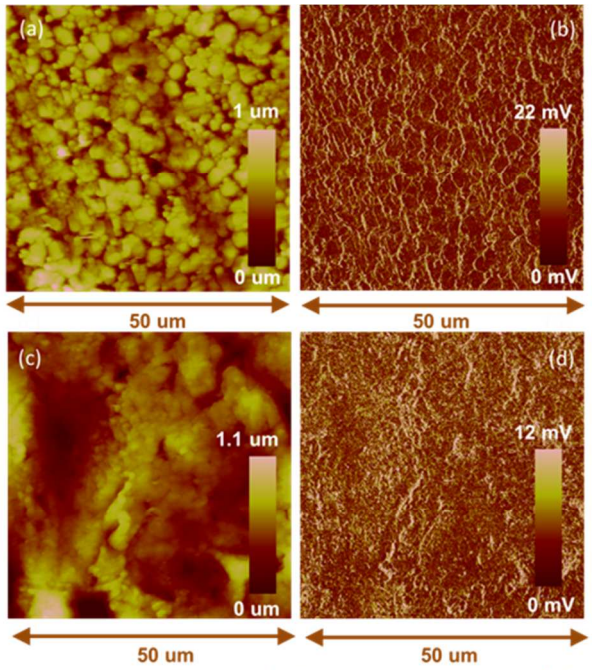

Fig. 3 Topography and PFM amplitude images for samples quenched at (a, b) -20 ºC and (c, d) 100 ºC, respectively.

The self-polarisation of the β-phase in PVDF films has also been verified by the piezoelectric effect based voltage generation. Figure 4(c, d) shows the voltage response for samples quenched at -20 ºC and 100 ºC, measured using impact testing. For the preparation of microgenerators, the film samples were enclosed in 100 µm thin Cu films and further sealed using non-permeable polyurethane films. The samples were tested under a a 100 N peak impact load using an Instron Dynatup 9200 test rig with the open circuit voltage being measured directly on an oscilloscope. The PVDF films quenched at -20 ºC show a voltage output of ~3V, nearly three times higher than that of the device using the film quenched at 100 ºC. These results further confirm that the PVDF films consist of self-polarised β-phase crystal with the PVDF films quenched at -20 ºC displaying a much higher piezoelectric coefficient than other films. Moreover, the self-polarised β-phase films were found to be very stable over a long period of storage time and subsequent annealing (Fig. S2, SI). No appreciable change in the topography and morphology of the samples was observed with the d_{33} value remaining unchanged at -50 pm/V for samples stored at ambient conditions. After annealing the d_{33} value was reduced to -43 pm/V; due to the temperature induced enhanced molecular mobility which can cause possible reorganisation within the crystal structure (Fig. S2, SI).[37]

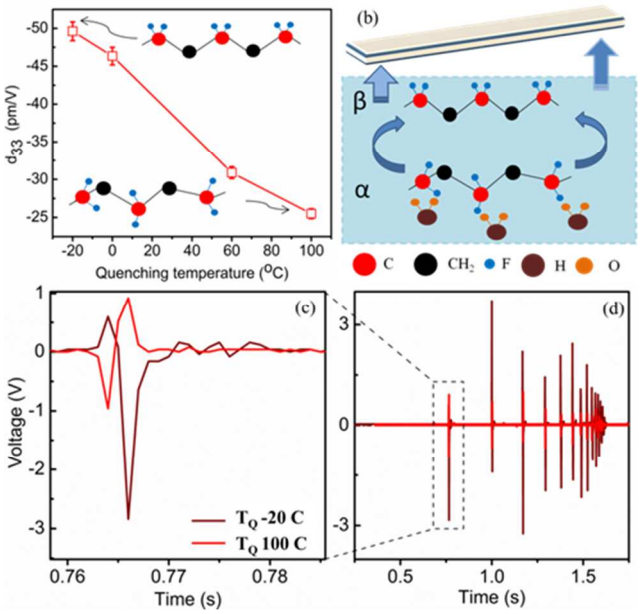

Fig. 4 (a) Variation of d_{33} as a function of T_Q, (b) proposed mechanism of sequential crystallisation and interaction with polar water molecules, (c, d) voltage output observed from microgenerators prepared using PVDF films quenched at -20 and 100 ºC.

The mechanism for the self-alignment of the β-crystals, however, is not entirely understood as yet. As an insulating glass substrate was used, and the thickness of the films is significantly large (>20 µm), the built-in electric field can be ruled out [22]. Fast quenching at low temperature induces a strong thermal field gradient, which can cause the crystals to align along the thermal field direction. The interaction with polar water can be one of the possible reasons for the alignment of the β-crystals[23,24]. The O-H groups of the water molecule can form hydrogen bonds with the C-F groups of PVDF leading to their orientation[23,24]. It has previously been observed that during the immersion of casting solution in non-solvent bath the mass exchange between the solvent and non-solvent is so fast that the liquid-liquid demixing takes places almost immediately, resulting in enhanced polymer concentration near the interfacial region. The conformation entropy changes occurring due to this increase in polymer concentration leads to better orientation and packing of CH_2-CF_2 dipoles leading to formation of the β-phase.[5] At low quenching temperatures, the crystallization is slow, which begins at the surface and proceeds towards inside of the film. As water is dipole molecule, the electric field acts at the initial surface, inducing aligned β-crystals, which in turn causes the alignment of the β-phase crystals in the sequential crystallization (Fig. 4(b)). First principle calculations by Bystrov et al have shown that interaction between

molecular chains of PVDF leads to the orientation of each molecular dipole moment along one direction parallel to the chain plane.[38] It is noteworthy that although β-phase crystals do not have preferential orientation in PVDF films formed by phase inversion[16] or by drying in air[12], the PVDF films obtained may still exhibit a certain degree of piezoelectric effect as shown by our results in Figure 3h. However, this aspect has been largely ignored in the literature with the porous PVDF films formed by phase inversion usually considered unsuitable for poling and electroactive applications. Nevertheless, our results clearly show that the temperature controlled phase inversion technique can be used to produce self-polarised, exclusive β-phase PVDF films with very high piezoelectric coefficient.

In conclusion, for PVDF films produced by phase inversion technique, the β-phase content increases rapidly with the reduction in quenching temperature, with nearly pure (~100%) β-phase obtained at -20 ^{o}C. The β-phase crystals are self-aligned and polarised, showing an abnormally high piezoelectric coefficient of up to -49.6 pm/V. The dense and homogeneous structure of PVDF films with relatively smooth and flat surface makes them particularly suitable for the electroactive applications. The process demonstrated here is simple and quick, with no further requirement for polarisation and demonstrates great potential for piezoelectric applications.

Notes and references

[a] Inst. Renew. Energy & Environ. Technol. Uni. of Bolton, Deane Road, Bolton, BL3 5AB, UK
[b] Ecole Superieure de Chimi de Monpellier, 8 Rue de I'Ecole Normale, 34090 Montpellier, France
[c] Dept. of Chem. & Mater. Eng., Uni. of Alberta, Edmonton, AB, T6G 2V4, Canada
[d] Dept. of Chem. Eng., Uni. of Birmingham, Birmingham B15 2TT, UK

The authors would like to acknowledge the partial financial support from the Engineering and Physical Sciences Research Council (EP/F06294X1). Materials support from Solvay Speciality Polymers is greatly acknowledged.

† Both authors contributed equally to the study

[1] A. Vinogradov and F. Holloway, Ferroelectrics, 1999, 226, 169.
[2] A. J. Lovinger, Development in Crystalline Polymers, Bassett, D. C. (ed.), Chpt.: "Poly(vinylidene) Fluoride", 1982, pp.195. ISBN: 978-94-009-7345-9
[3] J. Gomes and J. S. Nunes, V. Sencadas and S. Lanceros-Mendez, Smart Mater.Struct. 2010, **19**, 065010.
[4] H. R. Gallantree, IEEE Proc., 1983, **130**, 219.
[5] M. Zhang, A. Q. Zhang, B. K. Zhu, C. H. Du and Y. Y. Xu, J.Memb. Sci. 2008, **319**, 169.
[6] N. Soin, T. H. Shah, S. C. Anand, J. Geng, W. Pornwannachai, P. Mandal, D. Reid, S. Sharma, R. L. Hadimani, D. V.Bayramol, E. Siores, Energy Environ Sci. 2014, **7**, 1670
[7] T. Sharma, K. Aroom, S. Naik, B. Gill, J. X. Zhang, Ann Biomed Eng. 2013, **41**, 744.
[8] D. L. Polla, L. F. Francis, Annu. Rev. Mater. Sci. 1998, **28**, 563.
[9] A. Ballato, IEEE Proc. Ultrason. Symp., 1996, **13**, 575.
[10] P. Martins, A. C. Lopes, S. Lanceros-Mendez, Prog. Polym. Sci., 2014, **39(4)**, 683.
[11] R. Gregorio, J. Appl. Polym. Sci. 2006, **100**, 3272.
[12] D. Kim, H. S. Roh, Y. Kim, K. No, S. Hong, RSC Advances, 2015, **5(14)**, 10662.
[13] V.F. Cardoso, G. Minas, C.M. Costa, C. J. Tavares and S. Lanceros-Mendez. Smart Mater.Struct. 2011, **20**, 087002.
[14] X. F. Li, Y. G. Wang, X. L. Lu, C. F. Xiao, J. Membrane Sci. 2008, **320**, 477.
[15] A. Bottino, G. Camera-Rodab, G. Capannelli and S. Munari,J. Membrane Sci., 1991, **57**, l.
[16] M.C. Branciforti, V.Sencadas, S.Lacceros-Mendez, R.Gregorio, J. Polym.Sci. Part B Polym.Phys. 2007, **45**, 2793.
[17] J. H. Wendorff, J. Polym. Sci. Polym. Lett. 1980, **18**, 439.
[18] T. H. Young, L. P. Cheng, D. J. Lin, L. Fane and W. Y. Chuang, Polym. 1999, **40**, 5315.
[19] R. Gregorio and M. Cestari, J. Polym. Sci.: Part B: Polymer Physics, 1994, **32**, 859.
[20] M. G. Buonomenna, P. Macchi, M. Davoli, E. Drioli, Eur. Polym. J. 2007, **43**, 1557.
[21] Y. Ting, H, Gunawan, A, Sugondo and C. W. Chiu, Ferroelectrics, 2013, **446**, 28.
[22] M. Park, Y. Y. Choi, J. Kim, J. Hong, H.W. Song, T. Sung and K.S. No, Soft Matter, 2012, **8**, 1064.
[23] S.T. Chen, X. Li, K. Yao, F. H. Tay, A. Kumar, K. Zeng, Polymer 2012, **53**, 1404.
[24] B. J. Rodriguez, S. Jesse, S. V. Kalinin, J. Kim, S. Ducharme and V. M. Fridkin, Appl. Phys. Lett. 2007, **90**, 122904
[25] D. J. Kim, S. Hong, J. Hong, Y.Y. Choi, J. Kim, M. Park, T. Sung, K. S. No, J. Appl. Polym. Sci. 2013, **130**, 3842.
[26] M. Kanik, O. Aktas, H. S. Sen, E. Durgun and M. Bayindir, ACS Nano, 2014, **8**, 9311.
[27] S. Lanceros-Méndez, J. F. Mano, A. M. Costa & V. H. Schmidt, J. Macromolecul. Sci., Part B: Physics. 2001, **B40**, 517.
[28] B.E.Mohajir, N.Heymans, Polym. 2001, **42**, 5661.
[29] K.Nakagawa, Y.Ishida, J. Polym. Sci. Polym. Phys. 1973, **11**, 2153.
[30] C. Leonard, J. L. Halary, L. Monnerie and F. Micheron, Polym. Bull., 1984, **11**, 195.
[31] K. Loufakis and B. Wunderlich, Macromolecules, 1987, **20**, 2474.
[32] G. Teyssedre, A. Bernes and C. Lacabanne, J. Polym. Sci., Part B: Polym. Phys., 1993, **31**, 2027.
[33] Y. Choi, P. Sharma, C. Phatak, D. J. Gosztola, Y. Liu, J. Lee, B. Lee, J. Li, A. Gruverman, S. Ducharme, S. Hong, ACS nano, 2015, **9(2)**, 1809.
[34] K. Prashanthi, H. Zhang, V. R. Rao, T. Thundat, Physica Status Solidi (RRL)-Rapid Research Letters, 2012, **6(2)**, 77.
[35] S. V. Kalinin, A. Gruverman, Scanning probe microscopy: electrical and electromechanical phenomena at the nanoscale (Vol. 1), 2007, Springer Science & Business Media.
[36] C. Sun, J. Shi, D. J. Bayer, X. Wang, Energy Environ. Sci. 2011,**4**, 4508.
[37] M.P. Silva, C. M. Costa, V. Sencadas, A. J. Paleo, S. Lanceros-Mendez, J. Polym. Res. 2011, **18**,1451.
[38] V. S. Bystrov, N. K. Bystrova, E. V. Paramonova, G. Vizdrik, A. V. Sapronova, M. Kuehn, H. Kliem and A. L. Kholkin, J. Phys.: Condens. Matter., 2007, **19**, 456210.

